JGR Oceans

RESEARCH ARTICLE
10.1029/2022JC019407

Tracing Oceanic Sources of Heat Content Available for Atlantic Hurricanes

E. A. Harris[1,2], R. Marsh[1], and J. P. Grist[3]

[1]School of Ocean and Earth Science, University of Southampton, Southampton, UK, [2]Ariel Re, Hamilton, Bermuda, [3]National Oceanography Centre, Southampton, UK

Key Points:

- 20%–40% of the warm water available in the Main Development Region (MDR) for Atlantic hurricanes in June is resident there 6 months previously
- Of the remaining warm water, which arrives from outside the MDR, 5%–15% arrives via the North Brazil Current
- Years of anomalous warmth in the MDR are associated with reduced arrival from outside the MDR and more local air-sea heat exchange

Correspondence to:
E. A. Harris,
elizabeth.harris@arielre.com

Citation:
Harris, E. A., Marsh, R., & Grist, J. P. (2023). Tracing oceanic sources of heat content available for Atlantic hurricanes. *Journal of Geophysical Research: Oceans*, *128*, e2022JC019407. https://doi.org/10.1029/2022JC019407

Received 29 OCT 2022
Accepted 29 MAR 2023

Abstract In the Main Development Region (MDR) for Atlantic hurricanes, the volume of water warmer than 26.5°C quantifies the potential source of energy for major storms. Taking a Lagrangian perspective, this warm water is backtracked on seasonal timescales in an eddy-resolving ocean model hindcast spanning 1988–2010. Being confined near the surface and assuming a mixed layer depth of 50 m, net heat fluxes into or out of water parcels advected toward the MDR are inferred from along-trajectory temperature tendencies. To first order, these heat fluxes match surface net heat fluxes during the months over which water advects into the region. Contributions to this warm water in the preceding 6 months include water resident in the MDR (20%–40%), arriving via the North Brazil Current (NBC, 5%–15%), or via Ekman drift across 10°S. In relative terms, decreased contributions from the NBC and Ekman drift and more in situ warming within the MDR lead to warmer, more active hurricane seasons.

Plain Language Summary More and stronger hurricanes can be maintained by a larger quantity of warm ocean water in the North Atlantic. This water can be tracked backwards through time in high resolution model data to see where it originated. While some of the warm water is already in the tropical Atlantic 6 months before the hurricane season, some moves into the area via ocean currents or is pushed northwards by local winds. More and stronger hurricanes are more likely to occur in years where there is less movement of water into the tropical North Atlantic, along with more local heating of the region in the months leading into the hurricane season.

1. Introduction

North Atlantic hurricanes continue to be a major cause of natural catastrophe damage and loss of life. The 2017–2021 seasons consistently produced damaging landfalling storms, driving the 5-year average annual economic loss in the US alone to 102.5 B USD (CPI-adjusted, NCEI, 2022), an unprecedented level. These years include the particularly damaging hurricanes Harvey, Irma, and Maria in 2017. Category 5 Michael in 2018 had the strongest recorded maximum windspeed for US landfall. Dorian decimated islands in the Bahamas in 2019. Six hurricanes made landfall in the US in 2020. Category 4 Ida hit New Orleans in 2021. 2022 brought Category 4 Ian to the west coast of Florida, the most damaging US hurricane since 2005. These active recent seasons have mainly occurred in years with anomalous warm water in the tropical North Atlantic (Figure 1).

Hurricane development requires an underlying heat source of water warmer than 26.5°C, combined with a low vertical wind shear atmospheric profile. This is in addition to an existing disturbance, atmospheric instability, and mid-level moisture to aid genesis of individual events (Demaria et al., 2001). McTaggert-Cowan et al. (2015) summarize work identifying the aforementioned temperature threshold as key to generating and sustaining hurricanes. Hence, a deep understanding of the oceanic heat sources necessary to support these storms is required to increase societal preparedness for possible disasters on seasonal and longer timescales.

The June monthly-mean anomalous volume of water warmer than 26.5°C in the North Atlantic north of 10°N is shown in Figure 1 along with annual hurricane count in the Atlantic basin. These metrics have a Pearson correlation coefficient of 0.43, statistically significant at the 99% level. This anomalous volume of warm water varies on multidecadal and interannual timescales, and is mainly negative prior to 1995, then generally higher after that. Peaks in the volume occur in 1998, 2005, 2010–2011 and 2016–2017, years with some of the highest hurricane counts.

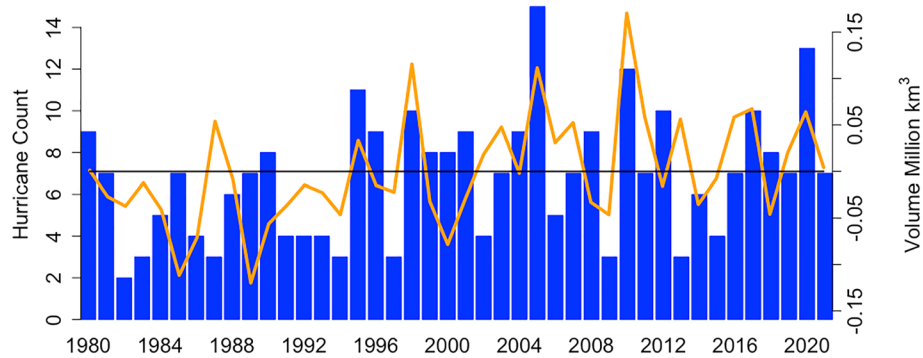

Figure 1. IBTrACS Annual North Atlantic Hurricane count (blue bars) and GODAS June volume anomalies of water warmer than 26.5°C in the Atlantic north of 10°N 1980–2021 (orange line). For GODAS volume anomalies, the black zero-line is aligned with the mean hurricane count.

Efforts continue to unravel the oceanic and atmospheric systems contributing to anomalous heat in the tropical North Atlantic. It has become clear that atmospheric heat flux plays a major role in heat transfer into the ocean on interannual timescales. Booth et al. (2012) found that variation in anthropogenic aerosols, modulating the incoming shortwave radiation, impacted North Atlantic sea surface temperate (SST) in a climate model. Dunstone et al. (2013) then linked this to tropical cyclone activity. Later studies (Watanabe & Tatebe, 2019) found that much of the anomalously cool North Atlantic SSTs observed in the 1970s and 1980s can be explained by increasing anthropogenic sulfate aerosols in climate model studies. Another source of aerosols into the atmosphere is volcanic activity, which Mann et al. (2021) suggest as the driver of multidecadal variability in Atlantic SST. Recent studies have confirmed the role of anomalous surface heating, and specifically a reduction of the oceanic latent heat loss in producing anomalous warm water in the tropical North Atlantic (Hallam et al., 2019; Harris et al., 2022).

While the role of air-sea heat flux in establishing Atlantic SST anomalies has been established in previous studies, heat transfer by ocean transport also plays a role in the development of Atlantic SST anomalies. Yan et al. (2017) argue that major hurricane frequency has increased since 2005, during which time aerosol concentration has been stable, while the Atlantic Meridional Overturning Circulation (AMOC) has weakened. A slowdown in the AMOC has been suggested to have driven anomalously positive Ocean Heat Content (OHC) in 2010, in contrast with 2017 when warming was attributed to changes in regional air-sea interaction (Hallam et al., 2019). R. Zhang et al. (2019) compile evidence for anomalous ocean heat transport divergence in the Atlantic, associated with changes in both the AMOC and Ekman dynamics which contribute to the changing circulation, notably in 2009–2010.

Different ocean currents feed into the Main Development Region for Atlantic hurricanes (MDR, Goldenberg et al., 2001, here defined as 10–20°N, 20–60°W). To the north of the MDR, the basin-integrated AMOC is monitored at 26°N, and comprises contributions from the Gulf Stream, mid and deep ocean, as well as Ekman transport (Cunningham et al., 2007). Seasonal variability is driven by basin-wide wind stress (Yang, 2015). The Ekman component was anomalously low in 2009–2010 (Smeed et al., 2018), allowing accumulation of heat in the MDR. The westward-flowing North Equatorial Current (NEC) traverses the southern MDR, while the eastward-flowing North Equatorial Counter Current (NECC) lies immediately to the south (Philander, 2001), and hence both potentially impact MDR temperature development. Amazon river outflow via the NBC has been proposed as a mechanism for hurricane intensification via a stratifying influence (Ffield, 2007). Despite the ground covered by these studies, the oceanic sources of warm MDR water in the lead up to the Atlantic hurricane season have not been examined collectively. This study aims to quantify transport into the MDR from these different regions in the lead up to the hurricane season, using a realistic high-resolution eddy-resolving ocean model hindcast.

Closing a heat budget for the MDR using Eulerian methods to quantify heat transport into this region via ocean transport is difficult due to disparate observational networks. Adopting a novel approach to investigating heat transfer into the MDR, we use the ARIANE particle tracking algorithm (Blanke & Raynaud, 1997), with data from the ocean model, to back-trace MDR warm water for 6 months. In a related study, ARIANE was used

with this model hindcast in the same region to forecast the drift of sargassum on seasonal timescales (Marsh et al., 2021). ARIANE is specifically used here to examine flows into the MDR that are associated with anomalously warm or cool hurricane seasons.

Data and methods will be described in more detail in the following section. Following this will be an investigation into the climatology of these oceanic pathways using model hindcast data to further understand the ocean dynamics in the study region. This will be compared with oceanic and atmospheric influences. Interseasonal variability will then be analyzed, to explain individual hurricane seasons. Finally, connections with Atlantic modes and mechanisms will be discussed, to link intraseasonal and interannual variability.

2. Data and Methods

We outline the various datasets used here to provide information on interannual variations in hurricane seasons and the associated warm water volume, and to obtain Lagrangian diagnostics. We further outline how the Lagrangian analysis is developed to partition waters inside and outside the MDR, to associate timescales to MDR arrival, and to infer (Lagrangian) heat fluxes along flow pathways for evaluation with (Eulerian) net surface heat fluxes.

2.1. IBTrACS

Atlantic basin hurricane count by year was compiled using the International Best Track Archive for Climate Stewardship (IBTrACS) (Knapp et al., 2010, 2018). Unique storms reaching greater than 64 knots of maximum wind speed were identified from this storm-centered point data which includes maximum winds at 6-hourly intervals over the ocean, more frequent near land, rounded to the nearest five knots.

2.2. GODAS

The observed volume of Atlantic water warmer than 26.5°C north of 10°N was calculated using the National Center for Environmental Prediction (NCEP) Global Ocean Data Assimilation System (GODAS) ocean reanalysis product (Behringer & Xue, 2004). This dataset contains gridded global potential temperature at 40 discrete depths, at 1/3° latitude and 1° longitude spacing, from 1980. While observations used to create this data are increasingly scarce with depth and further back in time, the data used in this study is near the surface and relatively recent.

2.3. NEMO Hindcast

A 1988–2010 hindcast model run was used to track particles. This dataset is output from the Nucleus for European Modeling of the Ocean (NEMO) ocean model (Madec, 2008), run in a high-resolution 1/12° eddy-resolving global configuration (ORCA12). Data used to compute trajectories comprise 5-day averages 3D ocean currents, temperature, and salinity; surface winds and net heat fluxes were used in further analysis.

NEMO-ORCA12 is forced with surface datasets produced by the DRAKKAR project (Brodeau et al., 2010), comprising 6-hourly mean 10-m winds, 2-m air temperature, 2-m humidity, daily mean radiative fluxes, and monthly-mean precipitation fields, adjusted from ERA40 reanalysis (Uppala et al., 2005). The hindcast used here is obtained with NEMO v3.2 and the following DRAKKAR Forcing Sets (DFS): DFS4.1 forcing up to the end of 2007, switching to NEMO v3.3.1 and DFS5.1.1 forcing in an extension to the end of 2010. Details of model parameterization and initialization are outlined in Blaker et al. (2015).

2.4. Lagrangian Analysis

The ARIANE package is used for tracing water parcels using the NEMO-ORAC12 model output data described above. Starting points are selected, and positions are saved at 5-day intervals up to 170 days. Start points on 30 June and 30 September are defined at grid points within the MDR where the temperature in the water column is greater than 26.5°C. Constraining the start points to the MDR allows for identification of movement of particles and heat transfer into this highly studied region intimately connected with hurricane development, at a temperature threshold identified as a minimum for sustaining hurricanes.

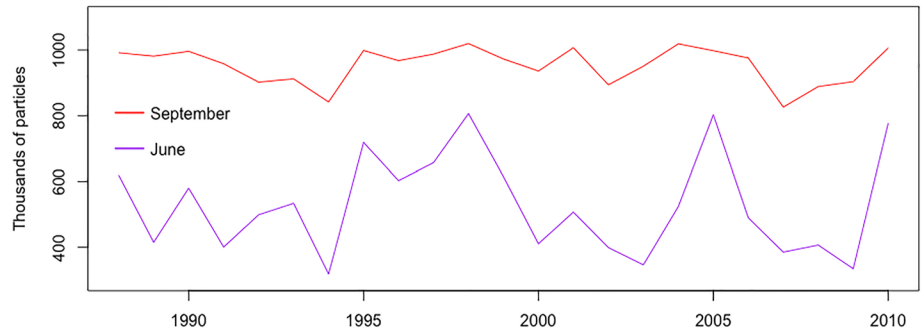

Figure 2. Number of particles initially warmer than 26.5°C in Main Development Region on 30 June (purple) and on 30 September (red).

The number of particles warmer than 26.5°C can be used as a proxy for heat content in the MDR. In Figure 2, this number is plotted for June and September of each year in the ORCA12 dataset. The variability in June is much greater than September. By September, most of the MDR SST particles are already warmer than 26.5°C. As a consequence, the amount of warm water in the MDR is less variable than in June. As the number of "warm water particles" in the MDR in June is indicative of MDR OHC, it is naturally linked to hurricane activity in the Atlantic Basin, with notable peaks in the active hurricane seasons 1995, 1998, 2005, and 2010 in Figure 1.

From the start points, ARIANE runs backwards (or forwards) to trace the path of the water parcels into (out of) the MDR, recording the tendencies of temperature and other properties along flow pathways. A forwards run from 30 June was run to quantify potential heat loss out of the region. Net heat fluxes, $Q_{\text{Lagrangian}}$, are inferred from temperature (T) tendencies between the 5-day output intervals (t, $t + Dt$, etc.), so $T(t + \Delta t) - T(t)$, for a representative mixed layer depth $h = 50$ m, as:

$$Q_{\text{Lagrangian}} = \rho C_p h \frac{T(t + \Delta t) - T(t)}{\Delta t}, \quad (1)$$

where ρ and C_p are respectively a representative density and the specific heat of seawater. The value of h is informed by a recent mixed layer climatology for the tropical Atlantic (Holte et al., 2017). Located midway between particle locations at arbitrary latitudes and longitudes, these heat fluxes are then averaged on a 0.5° grid along with mean age and other particle properties.

Figure 3 shows the tracks of a sample of particles at 1° spacing within the MDR and warmer than 26.5°C in September 2010, tracking particles backwards for 6 months. While the lengths of some particle tracks are contained within the MDR, longer tracks of faster moving particles are evident, clustered along the northeast coast of Brazil (NBC). The remainder of the particles move more slowly into the MDR across the southern boundary.

This Lagrangian approach to examining different routes of ocean heat transfer into the MDR is a novel methodology for investigating the variability of warm water available for hurricane development. The analysis reveals new insights into quantification of the sources of warm water flowing into this region and inter-seasonal variability leading to anomalously warm (cool) years in which the MDR heat content can support more (fewer) potentially damaging hurricanes.

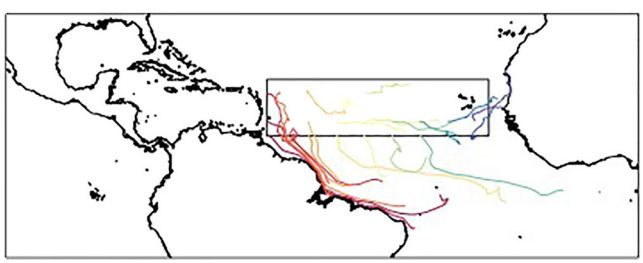

Figure 3. Sample of back-trajectories from September 2010, color-coded by particle id.

3. Results

Output from the three experiments: the particle back-trajectories from 30 June (BAC06) and 30 September (BAC09), as well as forward trajectories from 30 June (FOR06), are analyzed in the following sections. To understand the climatology of warm water transport into and out of the MDR, averages over the hindcast period of 1988–2010 are examined. This is demonstrated using monthly snapshots of the number of particles and average properties through the 6 months per 0.5° grid cell, including particle age and Lagrangian

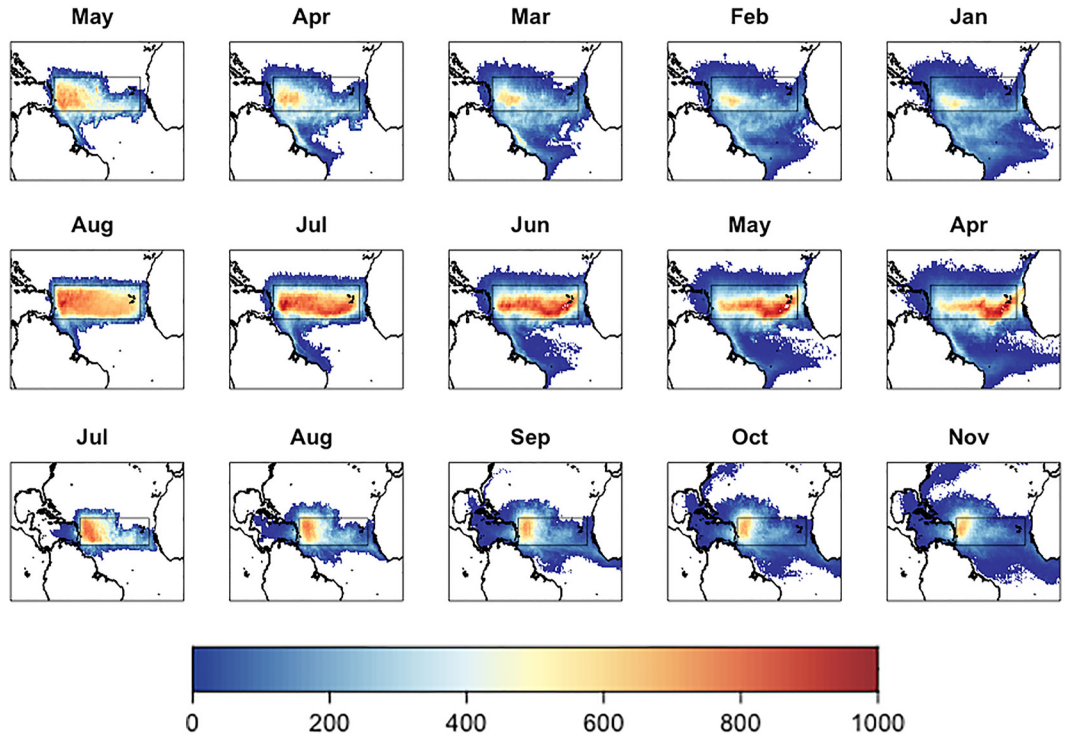

Figure 4. Number of particles per 0.5° grid cell at 1-month intervals from start date. Tracing particles that were in the Main Development Region (MDR) and warmer than 26.5°C on 30 June (top, tracing backwards), 30 September (middle, tracing backwards) and 30 June (bottom, tracing forwards). The MDR is outlined.

heat fluxes, which are compared with corresponding Eulerian surface heat fluxes from the hindcast. Mean ocean currents and wind stress are referenced as drivers of particle movement. Dynamics of heat transfer via ocean currents are then summarized schematically.

Individual years are compared to consider interannual variability, by identifying various source regions for water warmer than 26.5°C and quantifying the number of particles originating via individual pathways. The differences between particularly warm, active years in the dataset and cooler, inactive years are then examined, along with ocean currents and wind stress for those years, to highlight atmospheric and oceanic dynamics driving anomalously warm or cool conditions in the MDR that are of consequence for hurricane seasons.

Finally, we examine climate modes and mechanisms over the hindcast period, relating the variable development of MDR heat content via oceanic pathways to established analyses of tropical Atlantic variability.

3.1. Climatology of Oceanic Sources of Warm Water Into the Summertime MDR

In this section, the climatology of oceanic sources of water warmer than 26.5°C are discussed, by examining the backwards (forwards) trajectories of particles from 30 June and 30 September, for 170 days (approximately 6 months), to January or April (November) respectively. Particles in Figure 4 converge (diverge) gradually into (out of) the MDR with time along the backwards (forwards) trajectories.

In the top row, starting in June, and back-tracking 1 month earlier to May, particles are largely within the MDR, with some particles arriving via the NBC. In March, the NBC pathway is very clear along the north coast of Brazil. There is also a high density of particles visible south of 10°N in March, clearly to the north of the NBC. We can infer that these particles will move northwards more slowly than the NBC, due to their proximity to the MDR in March. In January, while the highest particle concentration is the MDR itself, particle origins are also well dispersed, from 10°S to 10°N, and largely west of 20°W.

The NBC also contributes to warm water particles residing in the MDR in September (middle row), though the local maximum in particle numbers in the eastern MDR in April is very pronounced, indicating far less

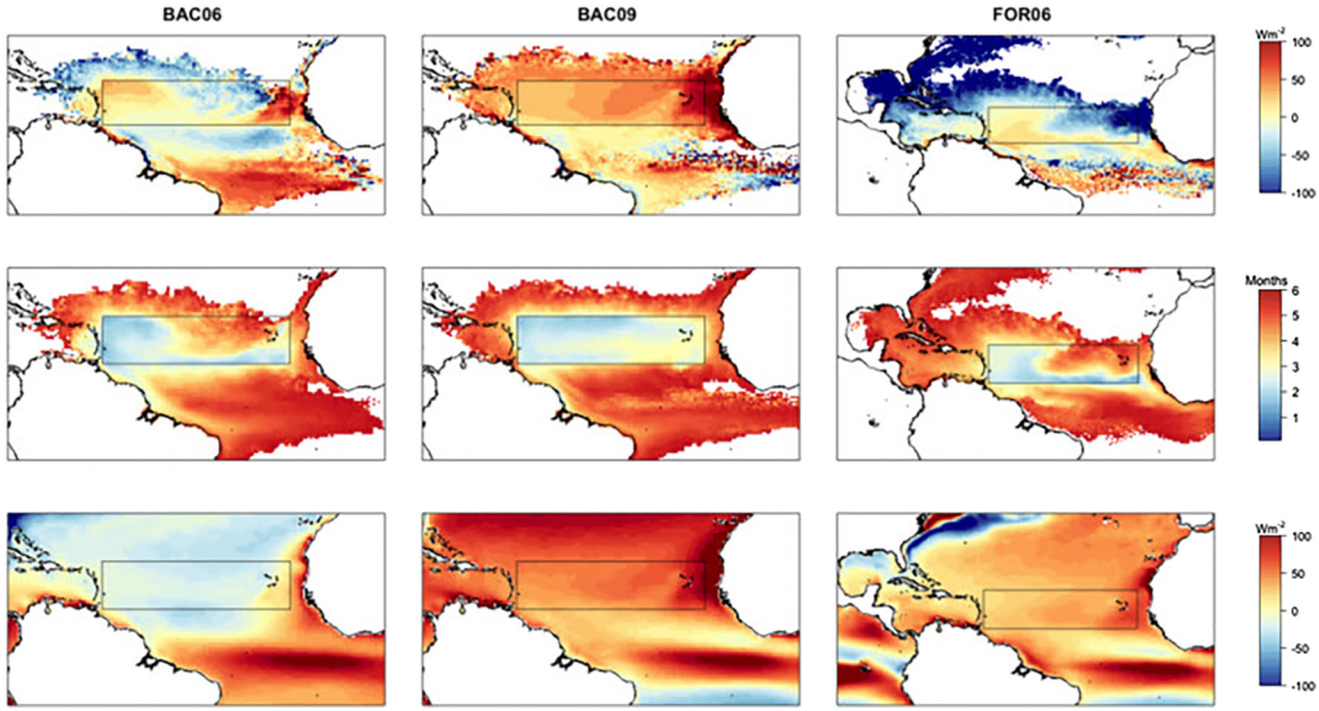

Figure 5. 1988–2010 ORCA12 mean heat flux (top row) and particle age (middle row) for ARIANE experiments, with mean Eulerian heat flux for the same 6-month period (bottom row).

movement into the MDR from other water sources over the spring and summer months. This suggests some westwards movement of particles within the MDR through this period.

To identify the extent to which warm water is being lost from the MDR via ocean currents, a forward run from 30 June is also undertaken (bottom row). Warm water particles move into the Gulf of Mexico in 2–3 months, some reaching the Gulf Stream by 4–5 months, along with general dispersal up to 10° to the north and south of the MDR.

While the Lagrangian analysis identifies the basic source regions of warm water, the particles also gain and lose heat along their track toward or away from the MDR, so the impact of ocean currents as heat sources or sinks cannot be isolated from air-sea heat flux, or Ekman dynamics, with this methodology. To elucidate this, the along-track heat flux via Equation 1, per 0.5° grid cell over the 6 months of each experiment, is plotted in the top row of Figure 5. The average particle age per experiment, in the middle row of Figure 5, is helpful for understanding the Lagrangian heat fluxes, as heat transfer processes are highly variable on intraseasonal timescales, with the ocean losing heat to the atmosphere in the northern hemisphere winter, and starting to gain heat from the atmosphere by early summer. As particle tracks begin in the MDR, and move quickly along the NBC into the MDR, this brings down the average particle age in these areas, but regions furthest from the MDR have an average age closer to the end of the experiment. Over the 6 months of BAC06, on the left, heat is gained in the MDR in May and June, off the west coast of Africa where cool water upwells due to offshore easterly trade winds, and south of the equator in January.

The Eulerian 6-month averaged heat flux (Q_{net}) in the left panel of the bottom row (averaged January to June) also shows general heat loss in the Atlantic north of 5°N, as this winter heat loss to the atmosphere in the northern hemisphere outweighs the heat gain in early summer, and heat gain south of this latitude, in the deep tropics, and for the upwelling area along the west coast of Africa.

In contrast, heat is gained over most of the particle tracks ending in September, in the middle column of Figure 5, which corresponds to April to September averaged Q_{net} on the bottom row (middle panel), as the ocean gains considerable heat from the atmosphere in the late spring and through the summer.

FOR06, on the other hand (right panels), shows heat loss where warm water particles move north, as they mix with cooler water and lose heat to the atmosphere, particularly via the Gulf Stream. Some heat is gained in June

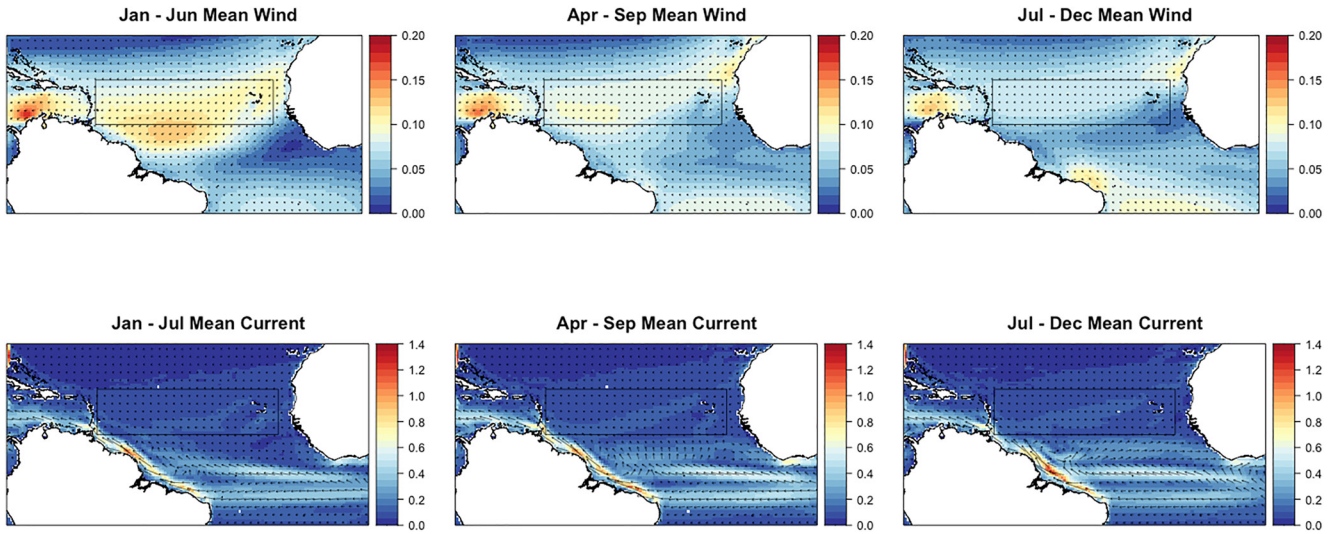

Figure 6. ORCA12 1988–2010 averages of 6-month means for wind stress (Nm^{-2}) and surface current (ms^{-1}). January–June corresponds to the time of BAC06, April–September to BAC09 and July–December to FOR06.

and July in the MDR and equatorial regions in November and December. Mean monthly Q_{net} for July to December (bottom right), shows mainly heat transfer into the ocean during the peak of summer and through the fall, with heat loss along the Gulf Stream as warm water moves quickly northwards.

The Lagrangian heat flux thus provides a complementary, time-varying perspective of ocean-atmosphere dynamics along flow pathways, contributing to the warm water pool available for hurricane development. This novel analysis reveals the role of oceanic pathways in the development of hurricane seasons, by highlighting heat transfer into the region in the months preceding the start of the Atlantic season, sourced within, or remote from, the MDR.

3.2. Climatology of Dynamical Influences on MDR Heat Content and Atlantic Hurricanes

In addition to seasonal change in Q_{net}, winds and ocean currents also vary seasonally, and contribute to varying mechanisms of heat transfer into the MDR through the year. Figure 6 highlights that winter/spring MDR wind stresses (top row) are stronger, leading to more mixing with cooler sub-surface waters and stronger advection. Weakening of wind stress through spring/summer subsequently favors heat accumulation in the MDR by September. The impact of the NBC (bottom row) will be examined in more detail on interannual timescales.

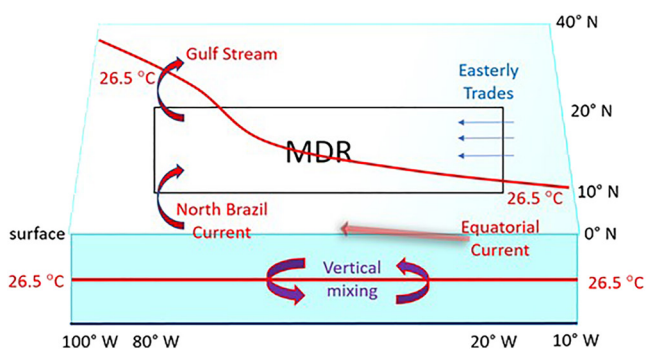

Figure 7. Physical mechanisms influencing ocean heat transport divergence in the Main Development Region (MDR) shown as arrows (see main text above for details).

Figure 7 depicts warm water pathways into and out of the MDR, as traced with particles, along with the atmospheric and oceanic drivers that contribute to heat content available for hurricane development. Ocean currents transporting water in and out of the MDR are identified as red arrows in this schematic. The Gulf Stream transports heat out of the region. The NBC bifurcates to partly flow into the MDR. The northern edge of the westward Equatorial Current crosses the southern boundary of the MDR. Variable Easterly trades (blue arrows) drive not only the Atlantic Niño signal, but also vertical mixing (purple arrows) across the 26.5°C isotherm. A combination of these dynamics and processes generates a larger or smaller pool of warm water, leading in turn to above or below average hurricane season activity. This warm pool is depicted by the red lines labeled 26.5°C.

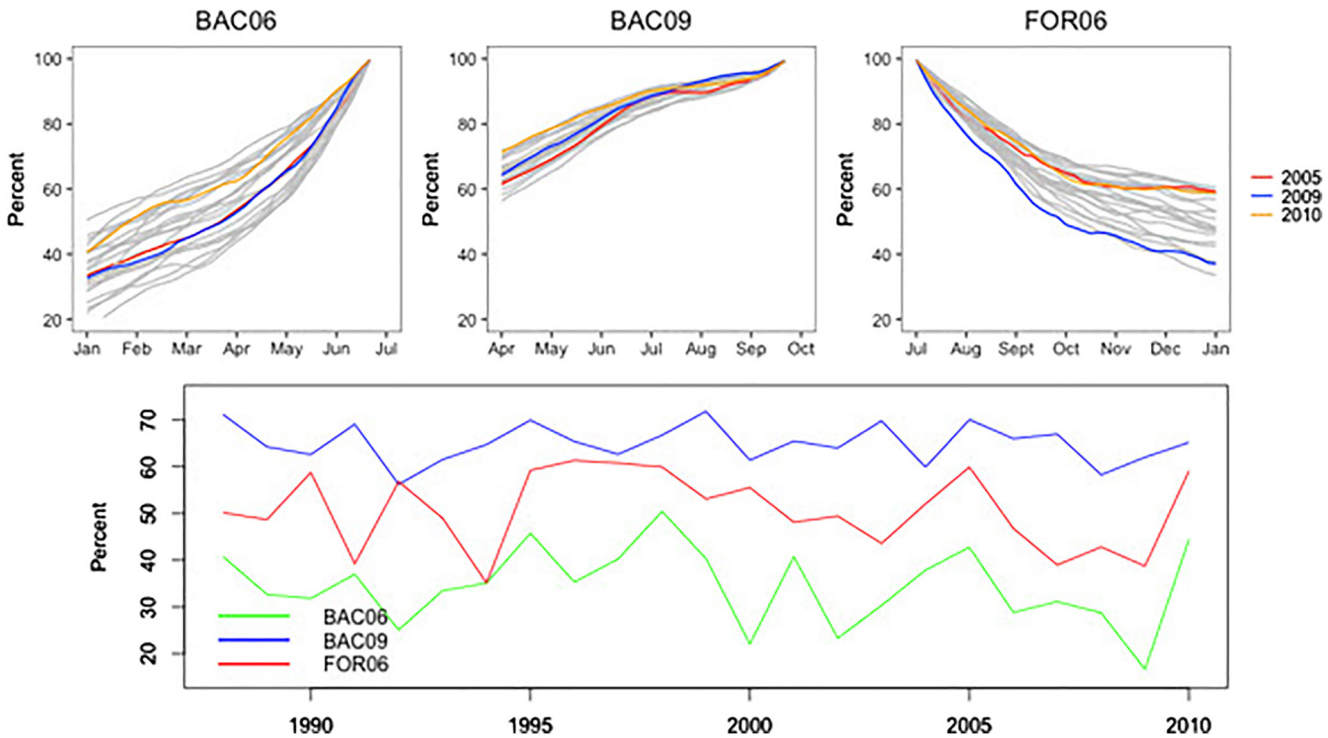

Figure 8. Percentage of particles in the Main Development Region (MDR) at each timestep that were in the MDR and warmer than 26.5°C at the start of the experiments, for each of the three experiments: BAC06, BAC09, and FOR06 by year (top panels). Time series of the percentage of these warm particles in the MDR at the end of the 6-month experiments (bottom panel).

3.3. Interseasonal Variability of Oceanic Pathways Into the MDR in Relation to Hurricane Activity

Section 3.1 considered average particle movement across the ORCA12 hindcast, introducing $Q_{\text{Lagrangian}}$ as a measure of net surface heat flux into the MDR for potential hurricane development. In this section, we develop Lagrangian diagnostics to compare mechanisms for oceanic heat transfer leading up to the start of the Atlantic hurricane season.

Figure 4 indicated that 6 months before the start of the hurricane season, many of the particles terminating in the MDR are already in situ in the MDR. This percentage of particles located within the MDR is plotted for each year, by experiment, in the top row of Figure 8. For BAC06, the MDR particle count quickly declines to a mean of 64% by month 2 of the experiment, associated with some of the faster moving pathways, though this varies between 52% and 77% by year. On average for these years in the dataset, 36% of the particles are in the MDR 6 months before the experiment start, varying between 17% and 50%.

Most of the particles from the start of the BAC09 (middle) experiment are in the MDR 2 months before the peak of the hurricane season, with a mean of 91% of the particles in the MDR at that time, and on average 65% of the particles in the MDR in April. Addressing heat loss from the MDR at the start of the hurricane season, in FOR06, on average 71% of particles are still in the MDR after 2 months from the experiment start time, and 51% by January, at the end of the experiment.

Comparing these experiments by start date, more heat exchange affecting the MDR heat content is via ocean currents from January to June (BAC06). From April to September (BAC09), more heat exchange affecting the MDR heat content is through in situ heat exchange from the atmosphere into the ocean.

The bottom panel in Figure 8 is a time series of the percentage of particles in the MDR at 6 months from the start of each experiment, essentially the "end points" 6 months earlier or later than the start time in the top row. This timeseries shows peak MDR "residency" for June-backtracked particles in 1995, 1998, 2005 and 2010; these are the years with the warmest MDR in June, and likewise, the most active hurricane seasons. There is a minimum in 2009, conversely a year with one of the lowest number of particles warmer than 26.5°C, during which only three

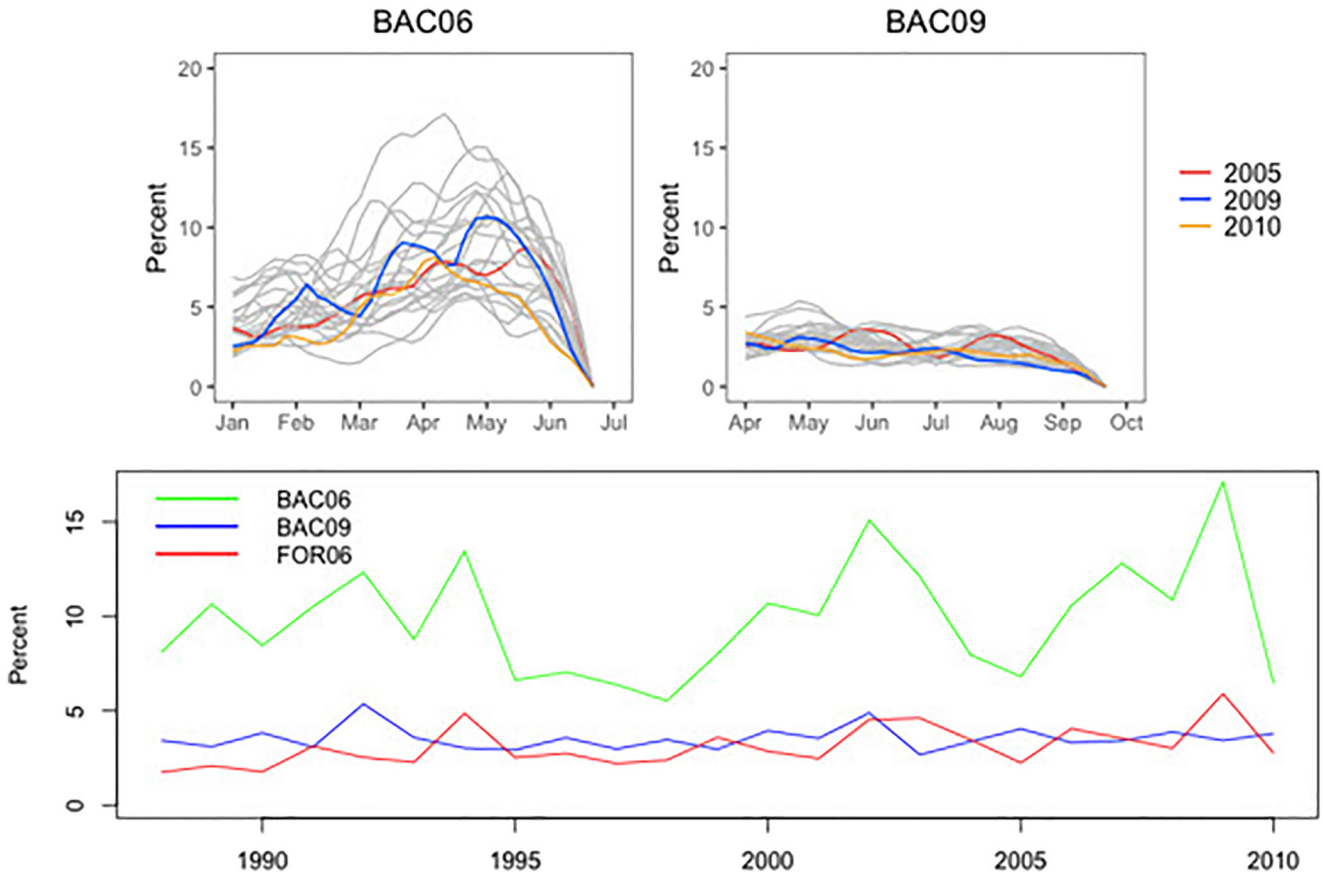

Figure 9. Percentage of particles in the North Brazil Current (NBC) at each timestep that were in the Main Development Region (MDR) and warmer than 26.5°C at the start of the experiments, for BAC06 and BAC09, by year (top panels). Time series of the percentage of these warm particles in the NBC at the end of the 6-month experiments (bottom panel).

hurricanes formed in the Atlantic basin. The number of particles in the MDR in January has a Pearson correlation coefficient of 0.78 with the number of particles in the MDR in June, and 0.55 with the annual Atlantic basin hurricane count, significant at the 99% level, suggesting a reasonable level of predictability for MDR heat content in June as well as seasonal basin-scale hurricane activity.

Apart from water resident in the MDR, a clear pathway for water moving into the MDR is the NBC, which is evident in the climatological analysis in Figure 4. To capture particles moving into the MDR via this current, Figure 9 shows the percent of particles in each year at each 5-day time timestep, south of 10°N, between 50 and 60°W. In BAC06, the greatest percentage of particles in this region is during March through May. Only a small percentage of particles is found in the NBC throughout BAC09, with variability by year for the 6 months of this experiment.

The time series in Figure 9 (bottom panel) shows the maximum percentage of particles in the NBC region at any time, rather than at the end of the experiment, recognizing that particles may pass through this region throughout the 6-month timespan. The BAC06 experiment maximum percentage of particles in the NBC timeseries is negatively correlated with the number of particles in the MDR in June, with a maximum in 2009, and minima in the active hurricane seasons. The Pearson correlation coefficient with the initial number of particles is −0.87 and with hurricane count is −0.61, significant at the 99% level.

We have quantified the contributions to warm MDR water coming from water in situ within the MDR 6 months prior to the start of hurricane season, and flow into the MDR via the NBC. The remaining water moving into the MDR moves north across the southern boundary primarily with Ekman drift. MDR warmth in June of warm years is largely in situ already by early/mid spring. This implies that warm years result from the accumulation of heat within the MDR (via surface fluxes), rather than transport of excess heat into the region from more equatorward regions. In cool years, an active NBC pathway accompanies suppressed MDR heat content. This is

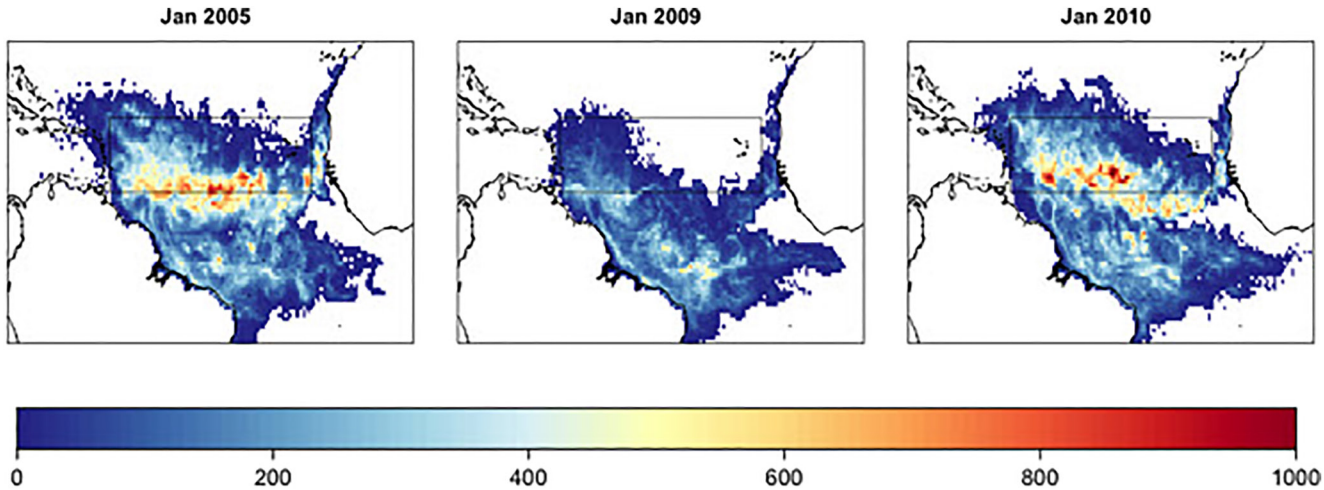

Figure 10. Number of particles per 0.5° grid cell in January which are in the Main Development Region and warmer than 26.5°C in June of the same year.

consistent with the relatively low heat gain or even heat loss that occurs in the along the main input pathway of the NBC (see Figure 5).

Three sample years were selected to examine oceanic and atmospheric dynamics leading to a smaller or larger than average number of warm particles in the MDR in June: 2005, 2009 and 2010. In 2005, there were a record number of 15 hurricanes, while only three hurricanes were recorded in 2009; in 2010, there were 12, well above the climatological average of 7 for 1980–2021 (Figure 1). For both 2005 and 2010, there is a relatively large number of warm water particles in the MDR in June. These 2 years are compared to see if similar antecedent conditions led to a larger warm pool in both years. In 2009, on the other hand, there is a relatively small number of particles in the MDR in June. In summary, around twice as many particles represent water warmer than 26.5°C in the MDR in 2005 and 2010, than in 2009 (Figure 2); comparing 2009 to 2010, we examine how antecedent conditions vary ahead of a cooler year and a warmer year, respectively.

Figure 10 shows the number of particles per 0.5° grid cell in each of these years from the BAC06 experiments. In 2005 and 2010, we note generally similar locations of particles 6 months earlier, in January. This suggests similar warm water pathways in the preceding months, with most particles residing in the MDR through this time, a contribution from the NBC, and the remaining particles drifting northwards across 10°N into the MDR. In contrast, warm waters in June 2009 originate mainly south of the MDR. These sample years demonstrate how warm years have more limited transport of water via ocean currents into the MDR, and more in situ warming within the MDR.

Oceanic and atmospheric conditions preceding June 2005 are compared with those prior to June 2010. We consider how Lagrangian motion and driving oceanic and atmospheric dynamics could potentially differ between these active hurricane seasons with large warm pools. Both years are characterized by negative wind stress anomalies across much of the region in the months preceding June (Figures 11a and 11e), although this is more strongly negative in 2010, particularly north of the MDR. Warm water in the MDR in 2005 therefore is more heavily influenced by Q_{net}, and in 2010 by Ekman dynamics, which other studies have also concluded (Hallam et al., 2019).

To consider how atmospheric and oceanic forcing may lead to cooler and warmer years in the MDR in June, we now compare the prevailing surface conditions in 2009 and 2010. Lower OHC in June 2009 is coincident with positive wind stress anomalies across the MDR through the preceding winter and spring (Figure 11c). The NBC and equatorial current are also anomalously positive in this period (Figure 11d). Wind stress anomalies, on the other hand, are negative in 2010, both in and around the MDR (Figure 11e).

This Lagrangian analysis of interannual variability of transport along pathways into the MDR, in the months preceding a hurricane season, confirms that increased transport from the south via the NBC and northwards Ekman drift across 10°S are associated with a smaller warm pool available for hurricane development by the start of the hurricane season; conversely, heat has more time to be exchanged via air-sea fluxes in years with less influential ocean transport.

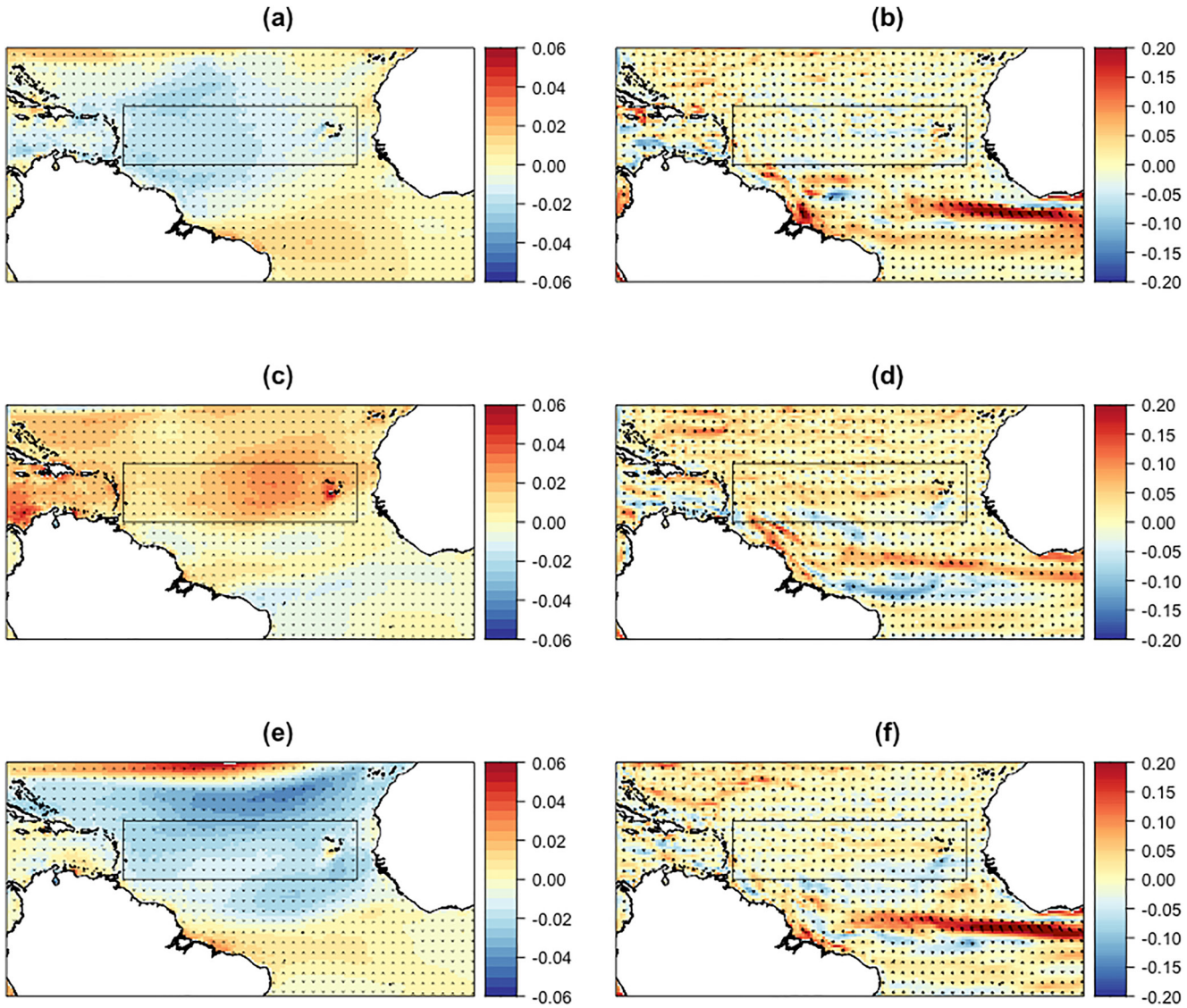

Figure 11. Mean January–June 2005 wind stress anomalies (Nm^{-2}) (a) and ocean current anomalies (ms^{-1}) (b) versus 2009 (c and d) and 2010 (e and f).

3.4. MDR Heat Content Linked to Modes of Climate Variability

Given the evidence for remote influences on MDR heat content, in particular the equatorial origin of warm water in the BAC06 experiments, and the more local MDR heating in BAC09 experiments, we examine regional patterns and time series of climate variability. Variability in tropical Atlantic temperatures and winds are evident on a range of timescales. Much of the variability can be quantified with two indices, which will be discussed in relation to the Lagrangian analyses and the associated volume of warm water available for hurricane development.

On interannual to decadal timescales, the Atlantic Meridional Mode (AMM) is the dominant statistical mode of tropical Atlantic SST variability (Chiang & Vimont, 2004; Servain et al., 1999). An index for the AMM is based on a leading dipole mode, associated with meridional SST gradient anomalies across the mean latitude of the intertropical convergence zone (ITCZ). When the AMM is in a positive phase, warm SST anomalies are centered at 10°N, with weak trade winds centered at 5°N.

A similar SST pattern to the Pacific El Niño had been observed in the tropical Atlantic, with a tongue of SST anomalies centered on the equator off west Africa (Lübbecke et al., 2018). This signal is formed in a similar fashion, as anomalous trade winds result in variations in coastal upwelling. A positive phase occurs when Atlantic trade wind strength is lower than average, allowing more warm water to pool across the eastern equatorial

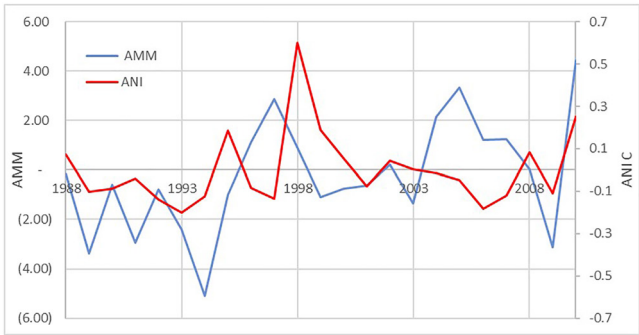

Figure 12. Atlantic meridional mode (AMM)-index (blue) and Atlantic Niño index (ANI) °C (red) 1988–2010 (Chiang & Vimont, 2004).

Atlantic. This results in positive feedback with trade winds over the area. The signal peaks in the summer and fall. An Atlantic Niño index (ANI) is calculated here from ORCA12 output by averaging SST anomalies over 3°N–3°S, 0°–20°W (following Zebiak, 1993).

The AMM-index is linked with hurricane activity (Vimont & Kossin, 2007) through warmer SST and low wind shear. The AMM-index (blue) in Figure 12 exceeds 2.0 in 1997, 2004, 2005, and 2010, with minima in 1994 and 2009. This is significantly correlated with hurricane count, with a Pearson correlation coefficient of 0.54, significant at the 99% level.

The ANI (Figure 12, red) is strongest in 1988, and also positive in 1995, 1999, and 2010, although notably fairly neutral in the very active hurricane seasons of 2004 and 2005. Regardless, the Pearson correlation coefficient with hurricane count for the years in this study is 0.49, significant at the 99% level.

The NBC has been discussed in previous sections in relation to inflow of water into the MDR. Transport via this current itself has been observed to exhibit variability on interannual and multidecadal timescales, in connection with AMOC variability (D. Zhang et al., 2011). However, though much of AMOC variability is buoyancy forced via the formation of North Atlantic Deep Water at higher latitudes, in this region, variability is largely wind-driven (Rühs et al., 2015).

In summary, the AMM index, AN, and NBC transport are mainly indicative of trade wind strength which is intimately tied to the development of warm water volume in the northern tropical Atlantic, and the MDR specifically. Changes in tropical circulation associated with larger-scale AMOC variability likely play a secondary role in the MDR heat budget.

4. Conclusions

Lagrangian techniques have been used to trace the origin of warm water into the MDR in the Atlantic hurricane season. A climatology is described using high resolution hindcast data spanning 1988–2010. This showed pathways into the MDR via the NBC, northwards flow across 10°N, and a component resident in the MDR 6 months earlier, which is more variable in June than September, when most of the near-surface MDR is above the 26.5°C threshold. On examining heat flux over the 6 months prior to the start of the hurricane season (backtracking experiment BAC06), heat is seen to be lost as water moves along much of these pathways toward the MDR; heat is conversely gained by waters within the MDR, particularly in the spring and summer (BAC09), which is associated with lower easterly wind stress in the region over the backtracking period.

Analysis of warm water source by year showed the variability between seasons, confirming that most of the heat in the MDR by June is resident in the MDR 6 months earlier, and a larger fraction in anomalously warm years with active hurricane seasons. The relative contribution of warm water from the NBC is hence smaller in these years, pointing to less transport from other potential remote heat sources, leading to anomalously warm and active seasons.

Examination of two warm years, 2005 and 2010, showed different dynamics in these years, with more negative wind stress anomalies in 2010 resulting in less transport into the MDR in connection with Ekman driven slowdown of the AMOC. Smeed et al. (2018) note increased heat transfer into the Atlantic due to this documented phenomenon, including higher sea level along US east coast, which would compound potential storm surge impacts if landfalling hurricanes were to occur in these conditions.

A comparison between a year with a high number of particles warmer than 26.5°C in the MDR in June (2010) and a year with a low number (2009) highlighted the increased transport in the cooler year across the southern boundary and into the MDR, including the NBC, driven by anomalously positive wind stress.

Further analysis could use similar methods to trace water north of the MDR backwards from September, to find origins of this larger Atlantic Warm Pool (Wang et al., 2011) in years when the Atlantic is anomalously warm, which is likely more variable than the MDR itself in the late summer.

Selected climate indices are significantly correlated with variability in the interannual contribution of MDR warm water sources. These indices are connected via trade wind strength and offer some insight into seasonal predictability of the climate system in this region. Predictions for the future also rely on understanding changes in surface heat flux, cloudiness, wind stress, and Ekman transport caused by climate change and variability. Wild (2016) predicts increasing brightness, which would increase atmospheric heat transfer into the ocean. To compound this, Caesar et al. (2021) conclude that the AMOC is weaker than it has been in the last 1,000 years, allowing more heat to accumulate in the MDR. These compounded trends are likely to increase MDR heat content further, if persisting into the future.

In summary, we have shown that warm MDR hurricane seasons are characterized by an anomalously large volume of warm water up to 6 months before the start of the hurricane season and relatively low advection of warm water into the MDR. The longer residency of water parcels in the MDR provides more time to be heated by air-sea fluxes, especially in the west of the MDR. Changes in the amount of warm water advected to the MDR are primarily associated with variability of pathways via the NBC and northwards Ekman drift, both of which are heavily dependent on tropical Atlantic wind stress. We have thus highlighted the relative importance of local and remote drivers of the seasonal warm water volume of the MDR, that in turn drives Atlantic hurricane activity.

Data Availability Statement

IBTrACS data is publicly available from the NOAA National Centers for Environmental Information (NCEI) website https://www.ncei.noaa.gov/products/international-best-track-archive. Likewise, GODAS data can be accessed from NOAA's Physical Sciences Laboratory https://psl.noaa.gov/data/gridded/data.godas.html. The hindcast NEMO-ORCA12 model datasets used in Ariane calculations are archived on a filesystem at the National Oceanography Centre, Southampton, and are available on request. The Ariane package developed by Laboratoire d'Océanographie Physique et Spatiale (LOPS) can be downloaded by registration: http://ariane.lagrangian.free.fr/ariane.html.

Acknowledgments
The NEMO-ORCA12 hindcast simulation was carried out by the Marine Systems Modelling group at the National Oceanography Centre (NOC). The version of ARIANE used here was developed by Dr George Nurser of NOC and implemented by Dr Jeff Blundell of the University of Southampton. AMM-index data is provided by http://www.aos.wisc.edu/~dvimont/MModes/Data.html.

References

Behringer, D. W., & Xue, Y. (2004). Evaluation of the global ocean data assimilation system at NCEP: The Pacific Ocean. In *Proc. Eighth symp. on integrated observing and assimilation systems for atmosphere, oceans, and land surface*. AMS 84th Annual Meeting, Washington State Convention and Trade Center.

Blaker, A. T., Hirschi, J. J. M., McCarthy, G., Sinha, B., Taws, S., Marsh, R., et al. (2015). Historical analogues of the recent extreme minima observed in the Atlantic meridional overturning circulation at 26 N. *Climate Dynamics*, *44*(1–2), 457–473. https://doi.org/10.1007/s00382-014-2274-6

Blanke, B., & Raynaud, S. (1997). Kinematics of the Pacific Equatorial Undercurrent: An Eulerian and Lagrangian approach from GCM results. *Journal of Physical Oceanography*, *27*(6), 1038–1053. https://doi.org/10.1175/1520-0485(1997)027<1038:kotpeu>2.0.co;2

Booth, B. B., Dunstone, N. J., Halloran, P. R., Andrews, T., & Bellouin, N. (2012). Aerosols implicated as a prime driver of twentieth-century North Atlantic climate variability. *Nature*, *484*(7393), 228–232. https://doi.org/10.1038/nature10946

Brodeau, L., Barnier, B., Treguier, A. M., Penduff, T., & Gulev, S. (2010). An ERA40-based atmospheric forcing for global ocean circulation models. *Ocean Modelling*, *31*(3–4), 88–104. https://doi.org/10.1016/j.ocemod.2009.10.005

Caesar, L., McCarthy, G. D., Thornalley, D. J. R., Cahill, N., & Rahmstorf, S. (2021). Current Atlantic meridional overturning circulation weakest in last millennium. *Nature Geoscience*, *14*(3), 118–120. https://doi.org/10.1038/s41561-021-00699-z

Chiang, J. C., & Vimont, D. J. (2004). Analogous Pacific and Atlantic meridional modes of tropical atmosphere–ocean variability. *Journal of Climate*, *17*(21), 4143–4158. https://doi.org/10.1175/jcli4953.1

Cunningham, S. A., Kanzow, T., Rayner, D., Baringer, M. O., Johns, W. E., Marotzke, J., et al. (2007). Temporal variability of the Atlantic meridional overturning circulation at 26.5◦N. *Science*, *317*(5840), 935–938. https://doi.org/10.1126/science.1141304

DeMaria, M., Knaff, J. A., & Connell, B. H. (2001). A tropical cyclone genesis parameter for the tropical Atlantic. *Weather and Forecasting*, *16*(2), 219–233. https://doi.org/10.1175/1520-0434(2001)016<0219:atcgpf>2.0.co;2

Dunstone, N. J., Smith, D. M., Booth, B. B. B., Hermanson, L., & Eade, R. (2013). Anthropogenic aerosol forcing of Atlantic tropical storms. *Nature Geoscience*, *6*(7), 534–539. https://doi.org/10.1038/ngeo1854

Ffield, A. (2007). Amazon and Orinoco River plumes and NBC rings: Bystanders or participants in hurricane events? *Journal of Climate*, *20*(2), 316–333. https://doi.org/10.1175/jcli3985.1

Goldenberg, S. B., Landsea, C. W., Mestas-Nuñez, A. M., & Gray, W. M. (2001). The recent increase in Atlantic hurricane activity: Causes and implications. *Science*, *293*(5529), 474–479. https://doi.org/10.1126/science.1060040

Hallam, S., Marsh, R., Josey, S. A., Hyder, P., Moat, B., & Hirschi, J. J. M. (2019). Ocean precursors to the extreme Atlantic 2017 hurricane season. *Nature Communications*, *10*(1), 1–10. https://doi.org/10.1038/s41467-019-08496-4

Harris, E., Marsh, R., Grist, J. P., & McCarthy, G. D. (2022). The water mass transformation framework and variability in hurricane activity. *Climate Dynamics*, *59*(3–4), 961–972. https://doi.org/10.1007/s00382-022-06169-5

Holte, J., Talley, L. D., Gilson, J., & Roemmich, D. (2017). An Argo mixed layer climatology and database. *Geophysical Research Letters*, *44*(11), 5618–5626. https://doi.org/10.1002/2017gl073426

Knapp, K. R., Diamond, H. J., Kossin, J. P., Kruk, M. C., & Schreck, C. J. (2018). International Best Track Archive for Climate Stewardship (IBTrACS) project. Version 4. [WP, NP, NA, SI, NI, SP].

Knapp, K. R., Kruk, M. C., Levinson, D. H., Diamond, H. J., & Neumann, C. J. (2010). The international best track archive for climate stewardship (IBTrACS) unifying tropical cyclone data. *Bulletin of the American Meteorological Society*, *91*(3), 363–376. https://doi.org/10.1175/2009bams2755.1

Lübbecke, J. F., Rodríguez-Fonseca, B., Richter, I., Martín-Rey, M., Losada, T., Polo, I., & Keenlyside, N. S. (2018). Equatorial Atlantic variability—Modes, mechanisms, and global teleconnections. *Wiley Interdisciplinary Reviews: Climate Change*, *9*(4), e527.

Madec, G. (2008). NEMO reference manual, ocean dynamics component: NEMO-OPA. Preliminary version. Note du Pole de modélisation, Institut Pierre-Simon Laplace (IPSL), France, 27, 1288-161.

Mann, M. E., Steinman, B. A., Brouillette, D. J., & Miller, S. K. (2021). Multidecadal climate oscillations during the past millennium driven by volcanic forcing. *Science*, *371*(6533), 1014–1019. https://doi.org/10.1126/science.abc5810

Marsh, R., Addo, K. A., Jayson-Quashigah, P. N., Oxenford, H. A., Maxam, A., Anderson, R., et al. (2021). Seasonal predictions of holopelagic sargassum across the tropical Atlantic accounting for uncertainty in drivers and processes: The SARTRAC ensemble forecast system. *Frontiers in Marine Science*, 1417.

McTaggart-Cowan, R., Davies, E. L., Fairman, J. G., Jr., Galarneau, T. J., Jr., & Schultz, D. M. (2015). Revisiting the 26.5°C sea surface temperature threshold for tropical cyclone development. *Bulletin of the American Meteorological Society*, *96*(11), 1929–1943. https://doi.org/10.1175/bams-d-13-00254.1

NOAA National Centers for Environmental Information (NCEI). (2022). U.S. billion-dollar weather and climate disasters. https://doi.org/10.25921/stkw-7w73. Retrieved from https://www.ncei.noaa.gov/access/billions/

Philander, S. G. (2001). *Atlantic Ocean equatorial currents* (pp. 188–191). Elsevier.

Rühs, S., Getzlaff, K., Durgadoo, J. V., Biastoch, A., & Böning, C. W. (2015). On the suitability of North Brazil Current transport estimates for monitoring basin-scale AMOC changes. *Geophysical Research Letters*, *42*(19), 8072–8080. https://doi.org/10.1002/2015gl065695

Servain, J., Wainer, I., McCreary, J. P., & Dessier, A. (1999). Relationship between the equatorial and meridional modes of climatic variability in the tropical Atlantic. *Geophysical Research Letters*, *26*(4), 485–488. https://doi.org/10.1029/1999gl900014

Smeed, D. A., Josey, S. A., Beaulieu, C., Johns, W. E., Moat, B. I., Frajka-Williams, E., et al. (2018). The North Atlantic Ocean is in a state of reduced overturning. *Geophysical Research Letters*, *45*(3), 1527–1533. https://doi.org/10.1002/2017gl076350

Uppala, S. M., Kållberg, P. W., Simmons, A. J., Andrae, U., Da Costa Bechtold, V., Fiorino, M., et al. (2005). The ERA-40 reanalysis. *Quarterly Journal of the Royal Meteorological Society*, *131*(612), 2961–3012. https://doi.org/10.1256/qj.04.176

Vimont, D. J., & Kossin, J. P. (2007). The Atlantic meridional mode and hurricane activity. *Geophysical Research Letters*, *34*(7), L07709. https://doi.org/10.1029/2007gl029683

Wang, C., Liu, H., Lee, S. K., & Atlas, R. (2011). Impact of the Atlantic warm pool on United States landfalling hurricanes. *Geophysical Research Letters*, *38*(19). https://doi.org/10.1029/2011gl049265

Watanabe, M., & Tatebe, H. (2019). Reconciling roles of sulphate aerosol forcing and internal variability in Atlantic multidecadal climate changes. *Climate Dynamics*, *53*(7), 4651–4665. https://doi.org/10.1007/s00382-019-04811-3

Wild, M. (2016). Decadal changes in radiative fluxes at land and ocean surfaces and their relevance for global warming. *WIREs Climate Change*, *7*(1), 91–107. https://doi.org/10.1002/wcc.372

Yan, X., Zhang, R., & Knutson, T. R. (2017). The role of Atlantic overturning circulation in the recent decline of Atlantic major hurricane frequency. *Nature Communications*, *8*(1), 1–8. https://doi.org/10.1038/s41467-017-01377-8

Yang, J. (2015). Local and remote wind stress forcing of the seasonal variability of the Atlantic Meridional Overturning Circulation (AMOC) transport at 26.5°N. *Journal of Geophysical Research: Oceans*, *120*(4), 2488–2503. https://doi.org/10.1002/2014JC010317

Zebiak, S. E. (1993). Air–sea interaction in the equatorial Atlantic region. *Journal of Climate*, *6*(8), 1567–1586. https://doi.org/10.1175/1520-0442(1993)006<1567:aiitea>2.0.co;2

Zhang, D., Msadek, R., McPhaden, M. J., & Delworth, T. (2011). Multidecadal variability of the North Brazil Current and its connection to the Atlantic meridional overturning circulation. *Journal of Geophysical Research*, *116*(C4), C04012. https://doi.org/10.1029/2010jc006812

Zhang, R., Sutton, R., Danabasoglu, G., Kwon, Y.-O., Marsh, R., Yeager, S. G., et al. (2019). A review of the role of the Atlantic meridional overturning circulation in Atlantic multidecadal variability and associated climate impacts. *Reviews of Geophysics*, *57*(2), 316–375. https://doi.org/10.1029/2019rg000644